Original Article

Characterization, thermodynamic parameters and *in vivo* antimalarial activity of inclusion complexes of artemether

Renu Chadha[1,*], Sushma Gupta[1], Geeta Shukla[2], Dharamvir S. Jain[3], Surjit Singh[4]

[1] *University Institute of Pharmaceutical Sciences, Panjab University, Chandigarh, India;*
[2] *Department of Microbiology, Panjab University, Chandigarh, India;*
[3] *Department of Chemistry, Panjab University, Chandigarh, India;*
[4] *Guru Nanak Dev University, Amritsar, Punjab, India.*

ABSTRACT: The present study aimed to improve solubility, dissolution and ultimate bioavailability of poorly soluble artemether, an antimalarial drug, by encapsulating it in β-cyclodextrin (β-CD) and its methyl and hydroxylpropyl derivatives. The effect of these complexes was confirmed by *in vivo* studies. Phase solubility studies indicated 1:1 stoichiometry and were supported by mass spectrometry and proton nuclear magnetic resonance (^{1}H-NMR) spectroscopy. True inclusion of artemether into the cyclodextrin cavity was observed in lyophilized complexes by differential scanning calorimetry (DSC), powder X-ray diffraction (PXRD) and Fourier transform infrared spectroscopy (FT-IR) studies. The mode of inclusion was supported by two-dimensional (2D) NMR. Solution calorimetry was used to confirm 1:1 stiochiometry by determining the enthalpy of interaction between the drug and cyclodextrins. The stability constant (K) of inclusion and other thermodynamic parameters such as enthalpy (ΔH) as well as entropy (ΔS) of binding accompanying the encapsulation were determined. The calculated value of K indicated that M-β-CD has maximum complexing efficiency. Dissolution studies indicated that the highest release rate was observed for lyophilized complexes. *In vivo* studies of lyophilized complexes of M-β-CD showed a 3-fold increase in antimalarial activity compared to artemether and resulted in 100% eradication of parasite. However, 83% and 50% survival rates were achieved in 40 days using HP-β-CD and β-CD complexes respectively. The study concludes that encapsulation of artemether by cyclodextrins is a good alternative to enhance the bioavailability of the drug.

*Address correspondence to:
Dr. Renu Chadha, University Institute of Pharmaceutical Sciences, Panjab University, Chandigarh 160014, India.
e-mail: renukchadha@rediffmail.com

Keywords: Artemether, β-cyclodextrins, inclusion complex, stoichiometry, *in vivo* studies

1. Introduction

Malaria is the most life threatening disease among parasitic infections. Of the four human malaria parasites, *Plasmodium falciparum* is the overwhelming cause of serious disease and death (*1*). Artemether, a rapidly acting antimalarial drug is potent, efficient against acute and severe *P. falciparum* malaria. WHO has listed it as an essential drug for the treatment of severe multiple resistant malaria (*2*). It acts by generating free radicals from the endoperoxy bridge of the drug and interacts with heme molecules located in the food vacuole of the parasite which is essential for its antimalarial activity (*3*). The therapeutic efficacy of artemether is greatly hampered due to its poor bioavailability and low aqueous solubility (*3*). One of the approaches to overcome these problems is to use cyclodextrins (CDs) as drug carriers. These oligosaccharides are most interesting because they form drug complexes in both the solution and solid state, wherein either the whole guest, or part of it (commonly the less polar part), is sequestered inside the hydrophobic cavity (*4*). The present study reports the preparation of inclusion complexes of artemether with β-CD (β-cyclodextrin), M-β-CD (methyl-β-cyclodextrin) and HP-β-CD (hydroxypropyl-β-cyclodextrin) and is aimed at improving its solubility and bioavailability. The data available regarding the formation of complexes of this important antimalarial drug (*3,5*) lack detailed characterization and thermodynamic parameters as well as *in vivo* studies except for one recent report (*6*) where the authors have used only HP-β-CD. Thus, the emphasis of the current study is both on formation of complexes and on an *in vivo* model to monitor the suitability of these complexes to enhance the bioavailability and dose of artemether.

2. Materials and Methods

2.1. *Preparation of artemether inclusion complexes*

The inclusion complexes of artemether with different types of CDs were prepared at a stoichiometric molar ratio of 1:1 using physical mixing, kneading and freeze-drying. Physical mixtures were prepared by simple mixing of drug with different CDs in a mortar. In the kneading method, cyclodextrins were wetted with water in a glass mortar until a paste was obtained, the drug was added and the slurry was kneaded for 90 min. An appropriate amount of water was added in order to maintain a suitable consistency. The product was dried under vacuum at 40°C for 48 h and sieved through 150 µm mesh. In the freeze-drying method, the required stoichiometric amount of drug was added to an aqueous solution of different CDs and solutions in the presence and absence of CDs were agitated on a magnetic stirrer for 24 h. The resulting solutions were frozen at (– 80°C) overnight. The products were lyophilized under 17.2 mTorr for 48 h. The sample was transferred into a vacuum desiccator and dried over silica gel under vacuum for at least 24 h.

2.2. *Characterization*

The complexes were characterized using a differential scanning calorimeter (DSC) (*7,8*), mass spectrometry, Fourier transform infrared spectrometry (FT-IR) (*9,10*), powder X-ray diffraction (PXRD) (*11,12*), proton nuclear magnetic resonance spectroscopy (^{1}H-NMR) (*13-15*) methods *vis-à-viz* phase solubility (*16,17*) and dissolution studies (*18*). Solution calorimetry was used to directly measure the enthalpy changes associated with encapsulation (*19,20*).

2.3. *Phase solubility studies*

Phase solubility studies were carried out according to the method described by Higuchi and Connors (*21*). These were performed by adding excess amounts of drug to 10 mL of simulated intestinal fluid (pH 6.8) solution in the absence or presence of increasing concentrations (0.001 to 0.015 M) of β-CD and M-β-CD and HP-β-CD. Suspensions were sealed and shaken in a water-bath shaker MSW-275 (Macroscientific Works, Delhi, India) at 37 ± 0.5°C for 24 h to ensure equilibrium. The samples were filtered through 0.45 µm Millipore filter paper and analyzed at 240 nm spectrophotometrically using a UV/VIS spectrophotometer (Perkin Elmer Lamda 15, USA). The presence of CDs did not interfere with the spectrophotometric assay of the drug.

2.4. *Differential scanning calorimetry (DSC)*

DSC thermograms of artemether, pure CDs and their inclusion complexes were obtained on DSC, Q20, TA instruments-Waters LLC, USA. The calorimeter was calibrated for temperature and heat flow accuracy using the melting of pure indium (mp 156.6°C and ΔH of 25.45 Jg^{-1}). The temperature range was from 25-350°C with a heating rate of 10°C per minute.

2.5. *Powder X-ray diffraction (PXRD) analysis*

Powder diffraction patterns of artemether and their inclusion complexes were recorded on an X-ray diffractometer (XPERT-PRO PANanalytical, Netherlands) using Cu as tube anode. The diffractograms were recorded under the following conditions: voltage 40 kV, 35 mA, angular range 5, fixed divergence slit.

2.6. *Mass spectrometry*

Mass spectrometric studies were performed using a Q-ToF quadruple time of flight mass spectrometer (Waters) equipped with an electrospray source. After optimization of the MS parameters, the spray voltage was set to 2.5 kV in the positive mode, and the heated metal capillary temperature was set at 80°C.

2.7. *Fourier transform infrared (FT-IR) spectroscopic studies*

The FT-IR spectra of artemether and inclusion complexes forms were recorded on an FT-IR spectrometer (Mode spectrum RXI, Perkin Elmer, UK) over the range 400-4,000 cm^{-1}. Dry KBr (50 mg) was finely ground in a mortar and samples of drug and their complexes (1-2 mg) were subsequently added and gently mixed. A manual press was used to form the pellets.

2.8. *Two-dimensional (2D) and proton nuclear magnetic resonance (^{1}H-NMR) spectroscopy*

^{1}H-NMR and two-dimensional (2D) COSY spectra in d_6-DMSO of artemether and inclusion complexes were recorded with a Brucker AC 300°C NMR spectrometer apparatus operating at 300 MHz using tetramethylsilane as an internal standard. For 2D COSY experiments, samples were equilibrated for at least 24 h.

2.9. *Solution calorimetry*

Isoperibol solution calorimeter (ISC) model 4300 (Calorimetry Science Corporation, Lindon, UT, USA) was used for thermal measurements. It is a semi-adiabatic calorimeter with temperature resolution, after noise reduction, close to 1 µK, which corresponds to a heat resolution of 1-4 mJ in a 25 mL buffer (pH 6.8) reaction vessel. The details are given in our previous

papers (*22,23*). The performance of the system was tested by measuring enthalpy of solution of potassium chloride (17.301 kJ/mol) in triple distilled water, which is in good agreement with known enthalpy of solution of 17.322 kJ/mol. The precision of any individual measurement was better than ± 0.03 kJ/mol for three consecutive experiments.

2.10. *Dissolution studies*

The dissolution studies were performed on the inclusion complexes of artemether prepared by all three methods using a USP (*12*) apparatus equipped with paddle type tribune at 50 rpm in 900 mL of simulated intestinal fluid (pH 6.8) pre-equilibrated at 37 ± 0.5°C. Inclusion complexes equivalent to 100 mg of artemether were filled into hard gelatin capsules. Sample was withdrawn at different intervals for a period of 4 h and analyzed spectrophotometrically at 240 nm. Three replicates were made for each experiment.

2.11. *In vivo studies*

2.11.1. *Parasite strain*

Plasmodium berghei (NK 65 strain) was used for evaluation of antimalarial activity *in vivo* studies and was maintained in BALB/c mice by intraperitoneal (*i.p.*) inoculation of infected blood. Percent parasitaemia was quantitated on every alternate day in Giemsa stained tail vein blood films and was calculated by counting at least 500 red blood cells (RBCs).

2.11.2. *Animals*

Four to five weeks old BALB/c mice (25-30 g) were procured and maintained in the Central Animal House and were provided with standard pellet diet and water *ad libitum*. Experiments were performed according to National Science Academy Guidelines Committee for the purpose of control and supervision of experiments on animals (CPC-SEA).The experimental protocol was approved by Institutional Animal Ethics Committee (A. I. E. C.).

Animals were divided into 2 major groups. Animals belonging to group I were used for dose standardization and animals of group II were used to monitor the efficacy and potency of prepared lyophilized complexes. Groups I and II were further subdivided as follows. Group I (56 animals) was subdivided into the following 7 groups (Table 1): Group IA, *P. berghei* infected animals (control); Group IB, animals treated with a single dose of artemether (4 mg/kg) on day 3 post inoculation (PI) up to 7 days; Group IC, animals treated twice a day with dose (5 mg/kg) on day 3 PI up to 7 days; Group ID, animals treated twice a day with dose (5 mg/kg) on day 2 PI for 3 consecutive days; Group IE, animals treated twice a day with dose (5 mg/kg) on day 2 PI for 7 consecutive days; Group IF, animals treated with dose (16 mg/kg) on day 1 PI, followed by a single dose (8 mg/kg) after 8 h and then two times a day up to 7 days; Group IG, animals treated with a single dose (10 mg/kg) after 8 h of PI followed by single dose therapy two times a day up to 7 days.

Animals of Group II were subdivided into 5 groups and each group comprised of 6 animals ($n = 6$). Artemether, Am-β-CD, Am-M-β-CD and Am-HP-β-CD were administered to group IIB, group IIC, group IID and group IIE respectively (Table 2). These were treated with single dose therapy (5 mg/kg) two times a day on 1 day of PI for 7 days.

2.11.3. *Preparation and administration of doses*

Artemether and its complexes were suspended in 0.5% carboxymethyl cellulose (CMC). Each animal was treated with 100 µL artemether and its various lyophilized complexes (Table 1).

2.11.4. *Challenge of the experimental animals and follow up of the experimental animals*

All the mice belonging to groups I and II were challenged with 10^6 *P. berghei* infected RBCs (*i.p.)*. After challenge the mean percent parasitaemia, percent activities of various complexes of artemether along with animal survivability were monitored.

Table 1. Dose standardization of antimalarial drug artemether in *P. berghei* infected mice ($n = 8$)

Groups	Artemether treated (mg/kg)*	Day of treatment	No. of survivals/ total No. of animals	Survival time ($t = 40$ days)
IA	0	NA	0/8	8 days
IB	4	SDT on day 3 PI up to 7 days	0/8	12-16 days
IC	5	TD on day 3 PI up to 7 days	0/8	15-18 days
ID	5	TD on day 2 PI up to 3 days	0/8	14-20 days
IE	5	TD on day 2 PI up to 7 days	2/8	40 days
IF	8	DD on day 1 PI followed by SD after 8 h. BD on day 2 PI up to 6 days.	5/8	40 days
IG	10	SD after 8 h PI followed by BD up to 7 days of infection	8/8	40 days

*Animals were treated with indicated amounts of artemether in 0.5% CMC.
Abbreviations: NA, not applicable; SDT, single dose therapy; TD, twice a day; DD, double dose; SD, single dose; PI, post inoculation.

Table 2. Antimalarial activity of complexes of artemether in *P. berghei* infected mice

Groups	Treatments	% Parasitaemia on day 8 PI	% Mortality ($n = 6$, $t = 40$ days)
IIA	0.5% CMC solution	35.56	100
IIB	Artemether (5 mg/kg)	4.9	66.7
IIC	Am-β-CD (5 mg/kg of Am)	4.6	50
IID	Am-M-β-CD (5 mg/kg of Am)	0.0002	16.7
IIE	Am-HP-β-CD (5 mg/kg of Am)	1.45	0

Abbreviations: *t*, No. of days; *n*, No. of animals per group; PI, post inoculation; Am-β-CD, artemether-β-cyclodextrins complex; Am-M-β-CD, artemether-methyl-β-cyclodextrins complex; Am-HP-β-CD, artemether-hydroxypropyl-β-cyclodextrins complex.

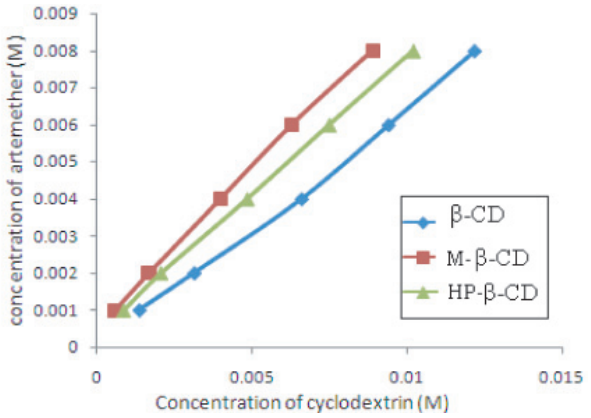

Figure 1. Phase solubility curves of artemether with β-CD and its derivatives at 37°C.

2.11.5. *Percent parasitaemia*

Percent parasitaemia was monitored on every alternate day for up to 40 days using tail blood smears, fixed in methanol and stained with Giemsa stain. At least 500 cells were counted.

2.11.6. *Statistical analysis*

Data was expressed as mean ± S.D. and parasitaemia of the artemether and its inclusion complexes were statistically assessed by one-way ANOVA followed by Turkey test using Jandel Sigma Stat 2.0 version. Differences were considered significant at $p < 0.05$.

3. Results and Discussion

3.1. *Phase solubility analysis*

The solubility of artemether increased in a linear fashion as a function of β-CD, M-β-CD and HP-β-CD concentration and followed an A_L-type system showing that a soluble complex was formed and no precipitation was observed over the entire concentration range studied. This linear host-guest correlation with a slope less than one suggested the formation of first order molar soluble complexes (Figure 1).

3.2. *DSC analysis*

DSC was used to provide detailed information about the physical state of the inclusion complex (Figure 2). The DSC thermograms of artemether were typical

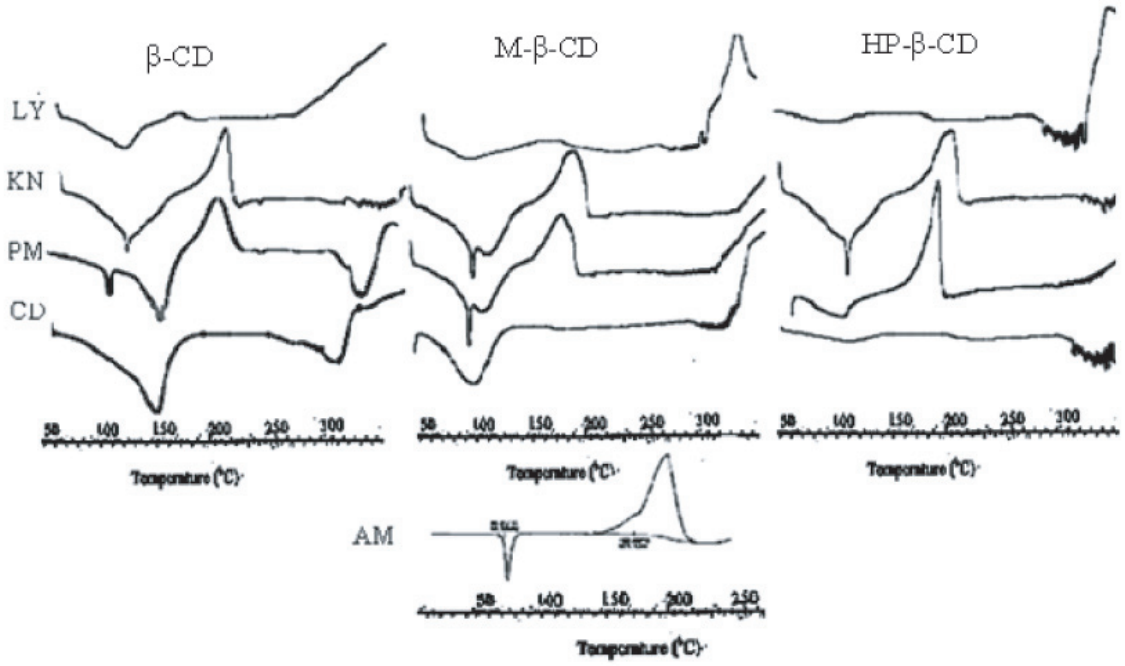

Figure 2. DSC thermograms of artemether-CD solid systems. AM, artemether; CDs, β-CD, M-β-CD and HP-β-CD; PM, physical mixtures; KN, kneaded complex; Ly, lyophilized complex.

of an anhydrous crystalline substance, exhibiting a sharp endothermic peak at 86.61°C, corresponding to the melting point of the drug. The complexes of the physical mixtures as well as the kneaded complexes of β-CD, M-β-CD, and HP-β-CD, and the phase transition thermal profile of artemether remained recognizable with reduction and broadening of the drug fusion peak, with a concomitant shift to lower temperature. The complete disappearance of the endothermic peak was observed for lyophilized systems indicating formation of a true inclusion complex. Decomposition was shifted to a higher temperature and was greatly reduced which further supports that the inclusion of the drug has enhanced its physical stability.

3.3. *PXRD analysis*

The diffraction pattern of artemether showed sharp diffraction peaks at 2θ° = 9.5622, 9.6787, 10.2706, 10.35353, and 19.3998 indicating its crystalline state and these were still detectable in the respective physical mixtures and kneaded complexes, though with evident reduction in their intensity. On the other hand, as expected the lyophilized products showed complete disappearance of drug diffraction peaks in M-β-CD, and HP-β-CD (Figure 3).

3.4. *Mass spectrometry*

The prepared lyophilized complexes of β-CD, M-β-CD, and HP-β-CD were introduced into the mass spectrometer and peaks were observed at m/z 1136, 1434, 1609, and 1679 corresponding to the charged $[\beta\text{-CD} + H]^+$, $[Am + \beta\text{-CD} + H]^+$, $[Am + M\text{-}\beta\text{-CD} + H]^+$, and $[Am + HP\text{-}\beta\text{-CD} + H]^+$, respectively, indicating 1:1 stoichiometry as suggested by phase solubility analysis (Figure 4). There is no trace of 1:2 stoichiometric complexes (*24,25*).

3.5. *FT-IR spectroscopic studies*

FT-IR could not give much useful information as the spectra of complexes of β-CD, M-β-CD, and HP-β-CD were found quite similar to their corresponding pure CDs because of the coincident absorption of both the host and guest molecules in most of spectral region. Bands of the included part of the guest molecule are masked by the bands of the spectrum of CDs (Figure 5).

3.6. *NMR spectroscopic studies*

NMR spectroscopy assures the existence of complexes in solution and also predicts its geometry by determining the chemical shift changes of drug protons due to its insertion into the hydrophobic cavity of cyclodextrins. A downfield shift in the cycloheptane protons H-d, H-g, H-h, H-m, and H-n of drug revealed the presence of artemether molecule in the cyclodextrin cavity (Figure 6B). The most plausible mode is that cycloheptane ring with endoperoxide group enters the cavity from

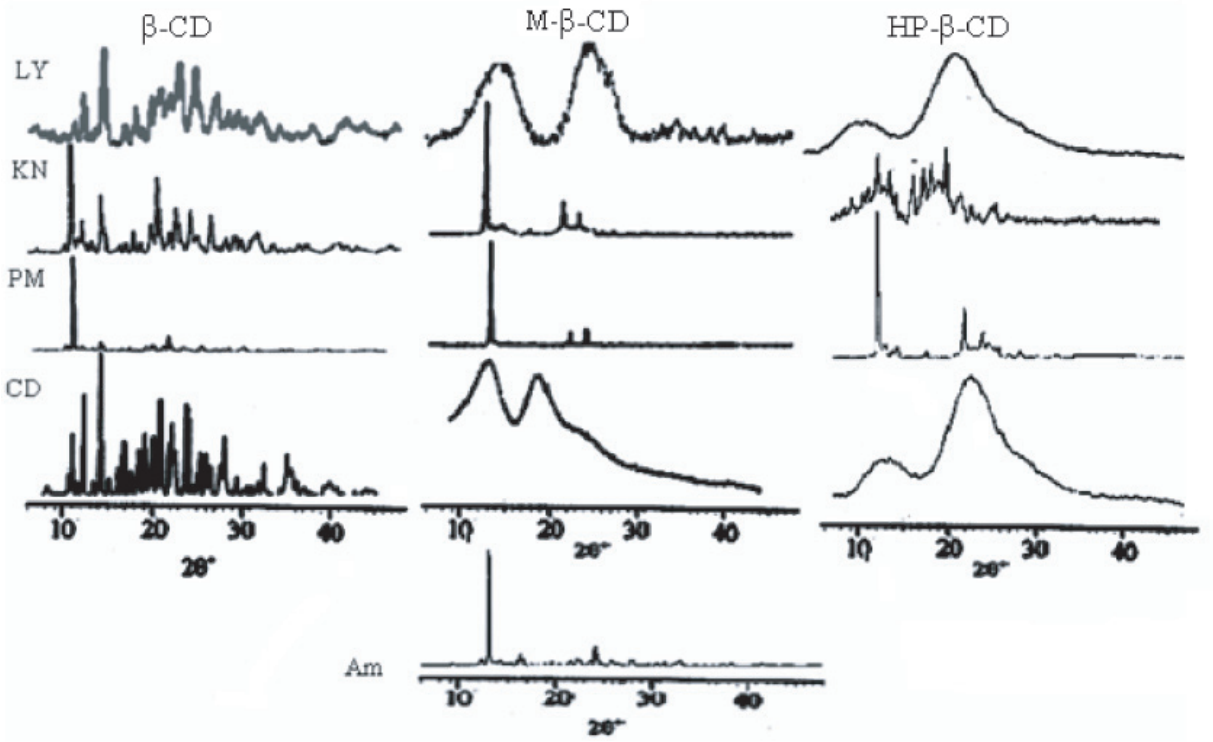

Figure 3. PXRD diffraction pattern of artemether-CD solid systems. AM, artemether; CDs, β-CD, M-β-CD and HP-β-CD; PM, physical mixtures; KN, kneaded complex; Ly, lyophilized complex.

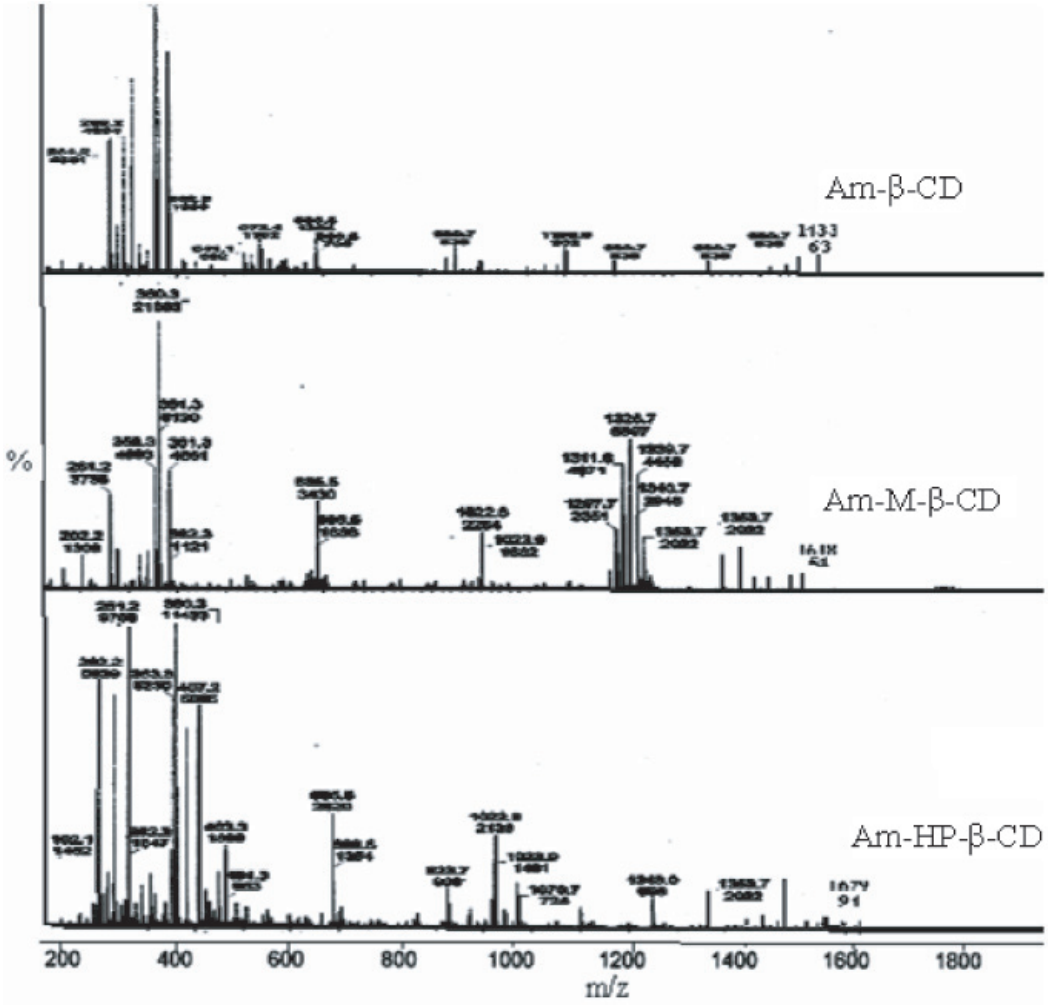

Figure 4. Mass spectra of lyophilized complexes of artemether.

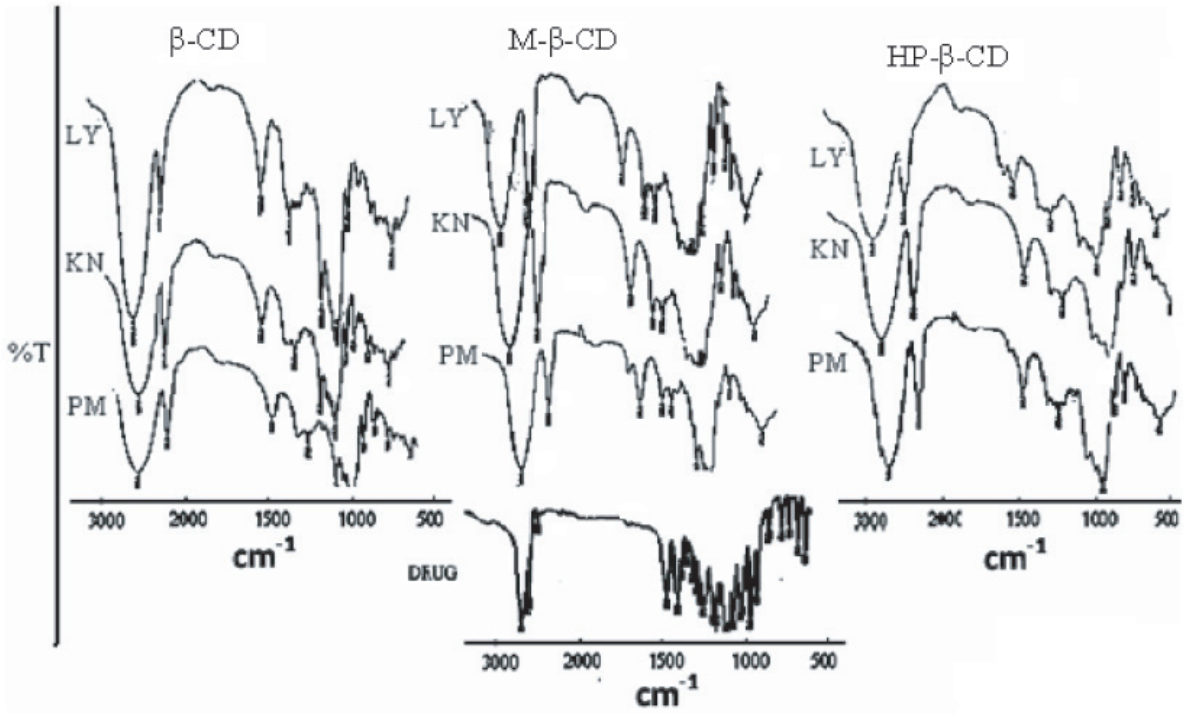

Figure 5. FTIR spectra of artemether-CDs solid systems. PM, physical mixtures; KN, kneaded complex; Ly, lyophilized complex.

the secondary face because of its narrower dimension (2.89 Å), whereas the opposite end of the molecule consisting of two cyclohexane rings with groups having dimensions of 6.9 Å is partially protruding (Figures 6A and 6C). A downfield displacement (Table 3) indicates that these protons are closer to the electronegative atom (oxygen) whereas, an upfield shift in protons H-e, H-b, and H-f of the molecule indicates variation in the local polarity due to weaker interactions with hydrogen atoms (shielding effect due to Van der Waals forces between drug and carbohydrates) (*26-29*). 2D COSY spectra were further used to get more insight into the geometry of the complex. It provides information about the spatial proximity between host and guest atoms by observing intermolecular cross-relations. The appearance of cross peaks (Figure 7) between H-5 protons of CD and H-b and H-n protons support our proposed inclusion mode involving insertion of the cycloheptane ring with endoperoxide bridge (trioxane ring) deep into the cavity. Cross peaks are also present between H-3 protons of CD and H-a protons of the oxygen containing cyclohexane ring of the drug. These results were in agreement with Yuen *et al.* and Illapakurthy *et al.* (*30,31*). However, it contrasts with findings obtained by Bo *et al.* (*6*). The encapsulation prevents decomposition leading to enhancement in physical stability as shown by DSC scans.

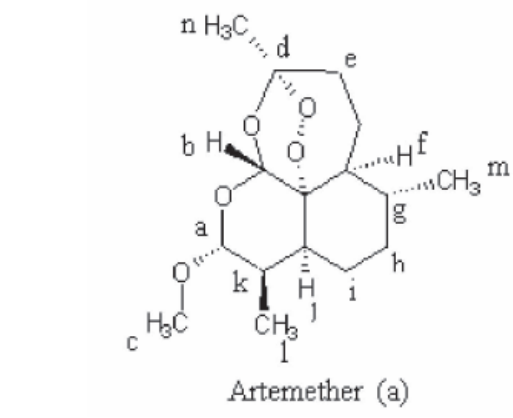

Figure 6. Chemical structure of artemether (a), inclusion mode of artemether with β-CDs (b), and molecular representation of inclusion complex of artemether with β-cyclodextrin cavity (c).

3.7. *Stoichiometry by solution calorimetry*

Solution calorimetry was employed to confirm the stoichiometry as well as to evaluate the stability constants and thermodynamic parameters associated with the binding process and are summarized in Table 4. The molar enthalpy of solution ($\Delta_{sol}H_{(M)}$) was found to be exothermic (– 13.18 kJ/mol) for artemether and was even more exothermic for the solution of artemether in the presence of CDs ($\Delta_{sol}H_{(M)(CD)}$). This is due to interaction between drug and cyclodextrins. Enthalpy of interaction was calculated by subtracting the enthalpy of solution of drug in cyclodextrins from that in pure buffer. The enthalpy of interaction was calculated from the equation 1:

$$\Delta H_{int(exp)} = \frac{\Delta H_{(CD)} - \Delta H}{v\,(l)} \qquad \text{(Eq. 1)}$$

where $\Delta H_{int(exp)}$ denotes enthalpy of interaction between drug and cyclodextrin per liter of solution; ΔH and $\Delta H_{(CD)}$ denote enthalpy of solution of drug in buffer and in buffered aqueous solution of cyclodextrins, respectively; and $v\,(l)$ denotes volume of sample cell in liters (0.025 L).

Enthalpy of interaction per mole of drug and cyclodextrin ($\Delta_{sol}H_{(M)}$) were calculated from equation 2:

$$\Delta H_{int(M)} = \frac{\Delta H_{int(exp)}}{a + b} = \frac{\Delta_{sol}H_{(M)(CD)} - \Delta_{sol}H_{(M)}}{1 + {X_2}/{X_1}} \qquad \text{(Eq. 2)}$$

where, a and b denote initial molar concentration of drug and cyclodextrin, respectively, in solution; X_1

Table 3. Values of ^{1}H chemical shifts before and after inclusion

Artemether	δ_{drug}	$\delta_{\beta\text{-CD complex, M-}\beta\text{-CD complex, HP-}\beta\text{-CD complex, respectively}}$	$\Delta\delta$ (ppm)
H-a	4.6845	4.8279, 4.5685, 4.5783	0.1434, – 0.116, – 0.016
H-b	5.3163	5.7255, 5.2974, 5.3003	0.4092, – 0.0189, – 0.1062
H-c	3.4023	3.3756, 3.2918, 3.2835	– 0.0267, – 0.1105, – 0.1188
H-d	2.1766	2.1853, 2.1681, 2.0437	0.0087, 0.02787, 0.01297
H-e	1.144	1.1519, 1.14068, 1.1574	0.0123, – 0.003327, – 0.00127
H-f, j	1.355	1.347, 1.34832, 1.3538	– 0.00802, – 0.0068, – 0.01336
H-g	2.3928	2.4014, 2.4051, 2.4032	0.00856, 0.0123, 0.0104
H-h	1.7731	1.7949, 1.7976, 1.6597	0.0218, 0.02446, – 0.01134
H-i	1.5938	1.5525, 1.6039, 1.5575	– 0.04132, 0.0101, – 0.03627
H-k	2.5073	2.5066, 2.5072, 2.5072	– 0.0007, – 0.0001, – 0.0001
H-l	0.8958	0.8905, 0.8928, 0.8445	– 0.00525, – 0.003, – 0.00545
H-m	0.8390	0.8400, 0.8423, 0.8949	0.00105, 0.0033, 0.009
H-n	1.2865	1.2933, 1.2944, 1.2946	0.0068, 0.0079, 0.0099

$\Delta\delta = \delta_{(complex)} - \delta_{(Free)}$.

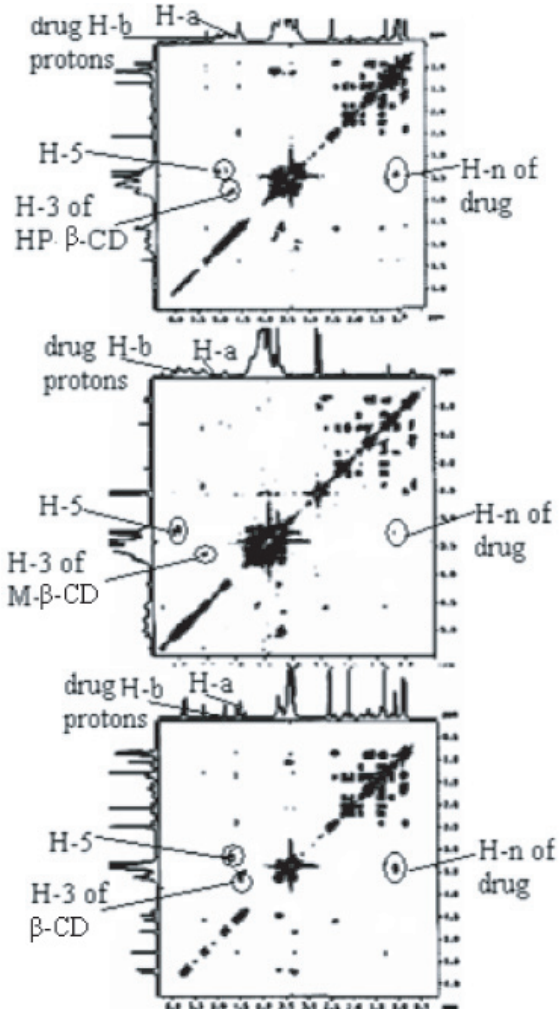

Figure 7. COSY spectra of inclusion complexes of artemether with β-CD, M-β-CD and HP-β-CD.

and X_2 denote apparent mole fractions of the drug and cyclodextrin, respectively, ignoring the concentration of buffers.

The detailed calorimetric results for artemether-β-CD complexation are summarized in Table 4. Similar calculations were obtained for M-β-CD and HP-β-CD.

The stoichiometry of the complex was ascertained utilizing a continuous variation method (Job's plot) (*32*) by plotting $\Delta_{sol}H_{(M)}$ *versus* X_2 (Figure 8). It is clear that the minima occurs at $X_2 = 0.5$ confirming the 1:1 stoichiometry as proposed by phase solubility, mass spectrometry, and proton NMR studies.

The thermodynamic constants were calculated assuming the following equilibria:

$$CD + \text{artemether} \leftrightarrow CD\text{:artemether} \qquad \text{(Eq. 3)}$$

The experimentally calculated enthalpy of interaction ($\Delta H_{int(exp)}$) is proportional to the product of molar concentration of the CD:artemether complex (c) in solution at equilibrium and enthalpy of binding per mole of drug ($\Delta H°$).

$$\Delta H_{int(exp)} = \Delta H° \times c \qquad \text{(Eq. 4)}$$

The equilibrium constant for equation 3 can be represented by

$$K = (c)/(a - c)(b - c) \qquad \text{(Eq. 5)}$$

The concentration of complex corresponds to equation 6.

$$c = [A - \sqrt{\{(A)2 - 4ab\}}]/2 \qquad \text{(Eq. 6)}$$

where, $A = a + b + 1/K$. Putting equation 6 in equation 4,

$$\Delta H_{int(exp)} = \Delta H° \times [(A - \sqrt{\{(A)2 - 4ab\}})/2] \times v \qquad \text{(Eq. 7)}$$

The binding constant K and enthalpy of binding ($\Delta H°$) were computed from the experimentally calculated enthalpy of interaction ($\Delta H_{int(exp)}$). The calculations were done by our computer program utilizing an iterative non-linear least square regression method to minimize the value of $\Sigma(\Delta H_{int(exp)} - \Delta H_{int(calc)})^2$ and are summarized in Table 5.

The values of free energy of inclusion ($\Delta G°$) and entropy of inclusion ($\Delta S°$) were calculated from the

Table 4. Interaction enthalpy of inclusion complexes of artemether with β-CD at pH 6.8

X_2	M_{AM} (mM)	$M_{β\text{-}CD}$ (mM)	$\Delta_{sol}H_{(CD)}$ (J)	$\Delta_{sol}H_{int(exp)}$ (J/L)	$\Delta_{sol}H_{int(M)}$ (kJ/mol)
0.895595	0.410704	3.5496	– 0.23773	– 4.09495	– 1.034
0.80532	0.8552	3.5376	– 0.45245	– 6.82378	– 1.5534
0.6407	0.712095	1.2698	– 0.32635	– 3.66651	– 1.85
0.71212	0.76508	1.89252	– 0.38802	– 5.43479	– 2.045
0.5849	0.62684	0.88316	– 0.28864	– 3.28199	– 2.1735
0.50453	0.8888	0.90536	– 0.40355	– 4.42512	– 2.4664
0.4398	1.1804	0.9267	– 0.50879	– 4.79028	– 2.2734
0.38254	1.5302	0.948	– 0.62668	– 4.89445	– 1.975
0.3249	0.806972	0.38836	– 0.31891	– 2.11813	– 1.772
0.2592	1.0769	0.3768	– 0.41172	– 2.27213	– 1.563
0.1865	1.6604	0.38062	– 0.61052	– 2.53189	– 1.2405
0.11131	1.488592	0.18644	– 0.52439	– 1.35142	– 0.8068
0.07896	2.2206	0.17534	– 0.76625	– 1.37599	– 0.5743

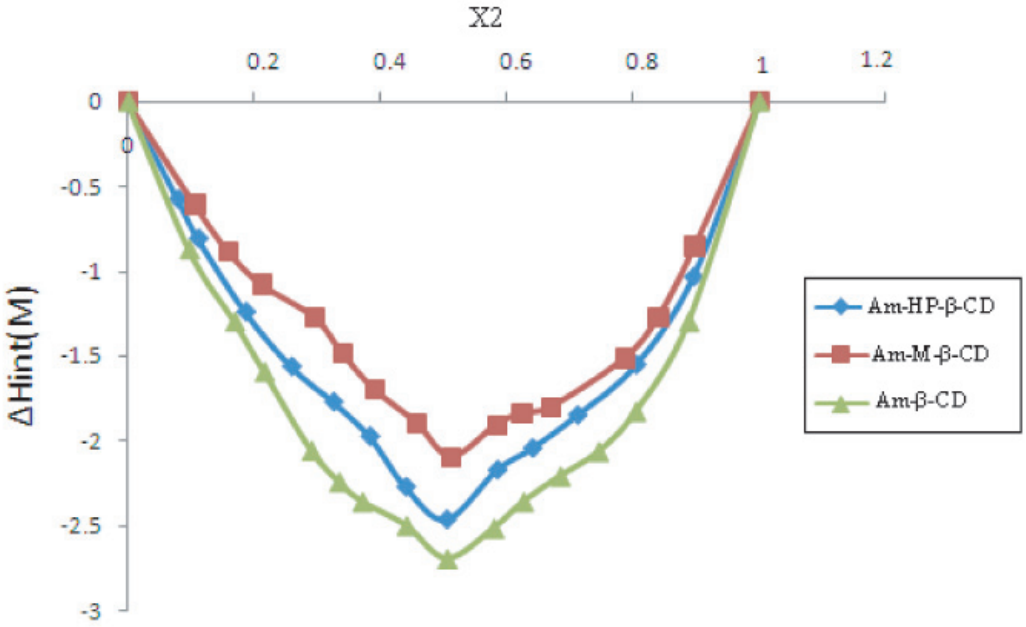

Figure 8. Plot of $\Delta H_{int(M)}$ *vs.* X_2 of β-CD, M-β-CD, and HP-β-CD of artemether (AM) at pH 6.8 in simulated intestinal fluid (SIF).

Table 5. Thermodynamic parameters of artemether with β-CD, M-β-CD, and HP-β-CD at pH 6.8 in SIF, determined using solution calorimetry

System	K (M^{-1})	ΔH° (kJ/mol)	ΔG° (kJ/mol)	ΔS° (J/mol•K)
Artemether + β-CD	1,175	–10.00	– 18.22	26.51
Artemether + M-β-CD	2,500	– 8.90	– 20.16	36.34
Artemether + HP-β-CD	2,440	– 11.8	– 20.10	26.78

following equations:

$$\Delta G° = – RT\ln K \quad \text{(Eq. 8)}$$
$$\Delta S° = (\Delta H° – \Delta G°)/T \quad \text{(Eq. 9)}$$

The values of K are between 1,100 to 2,500 M^{-1}, which is a favorable range for better bioavailability. Both enthalpic and entropic factors drive the inclusion process. The inclusion of drug was found to be an exothermic process while the entropy of reaction is positive in all these cases leading to values of Gibbs free energy (ΔG°) between – 18.2 to 20.2 kJ/mol. The magnitude of the equilibrium constant (K) indicates that both methyl-β-CD and HP-β-CD have nearly the same complex formation ability and which is further confirmed by dissolution and animal studies.

3.8. *Dissolution studies*

Rapid dissolution is the characteristic behavior of inclusion complexes but the comparative release of active material was strongly affected by the method of formulation. The lyophilized product exhibited the best dissolution properties and was followed by kneaded complex and physical mixtures (Figure 9). Moreover, the highest dissolution rate was found for M-β-CD complex followed by that of HP-β-CD and β-CD in simulated intestinal fluid (pH 6.8). The improvement

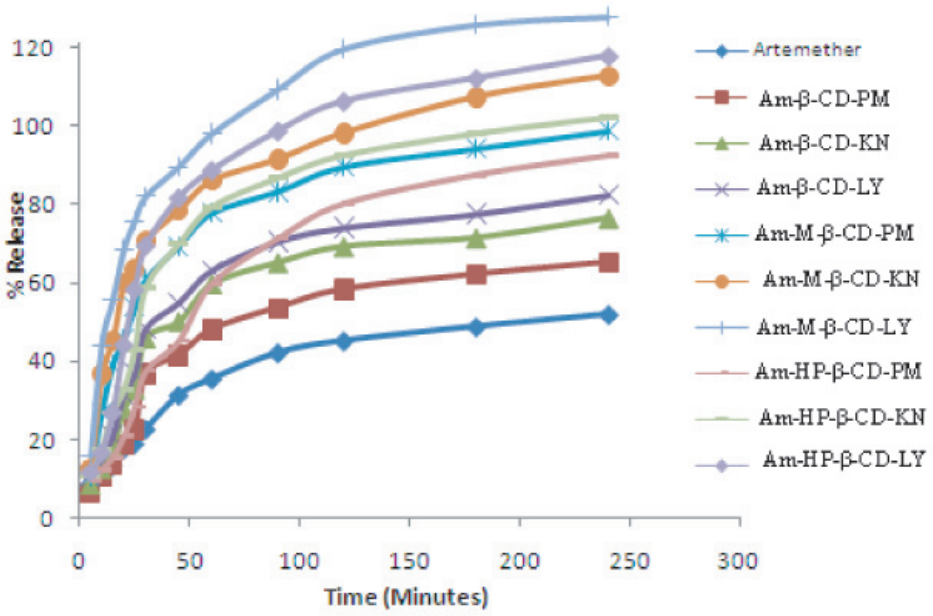

Figure 9. Dissolution profile of artemether and its complexes.

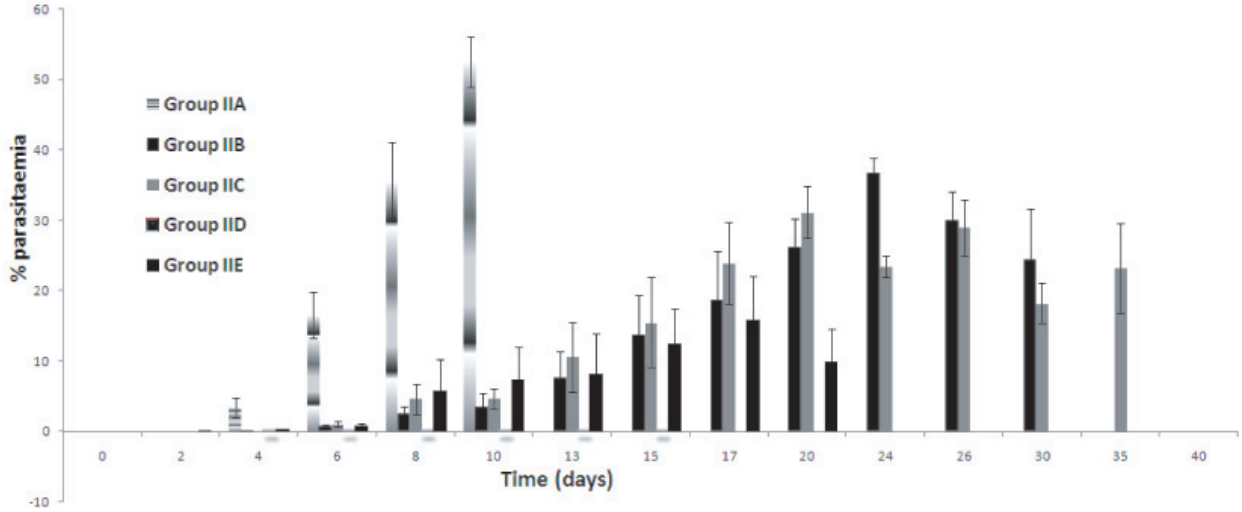

Figure 10. Percent parasitaemia observed in *P. berghei* infected mice (*n* = 6).

in the dissolution rate of lyophilized complexes may be attributed to the amorphous state of the active material, together with the increase in wettability and the solubility of the drug. Thus, the lyophilized complex with the highest dissolution rate is the most suitable product for animal studies.

3.9. *In vivo studies*

To monitor the protective efficacy of artemether and its inclusion complexes with β-CD complexes against *P. berghei* infection, dose standardization was carried out (Table 1). It was observed that artemether (Group IB) is insufficient to prevent mortality. However, survival time was increased (days 12-16) compared to control (day 8). Animals of Group IC, Group ID, and Group IE were treated with different dose therapies as given in experiment section and were again unable to eradicate the percent parasitaemia. Therefore, the dose was increased to 8 mg/kg and was started on day 2 PI. It was also found to be ineffective in preventing mortality. Then a dose of 8 mg/kg was given after 8 h of PI and treatment was continued up to 7 days. This treatment schedule was effective to eradicate the parasitaemia completely in 63% of animals. To achieve 100% survivality, the dose was again increased to 10 mg/kg and was continued for 7 days. Out of the entire tested doses the 5 mg/kg dose schedule was selected for the complexes to compare and differentiate them on the basis of their protective efficacy and potency compared to artemether.

The results are given in Table 2. It was observed that percent mortality rate with artemether alone, β-CD

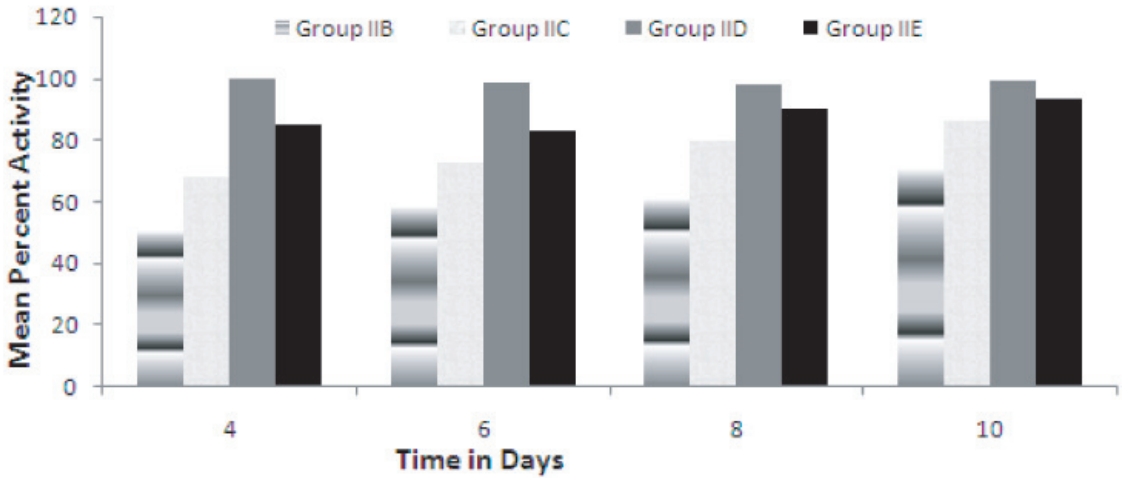

Figure 11. Antimalarial activity of lyophilized complexes of artemether in *P. berghei* infected mice (n = 6) as compared to control.

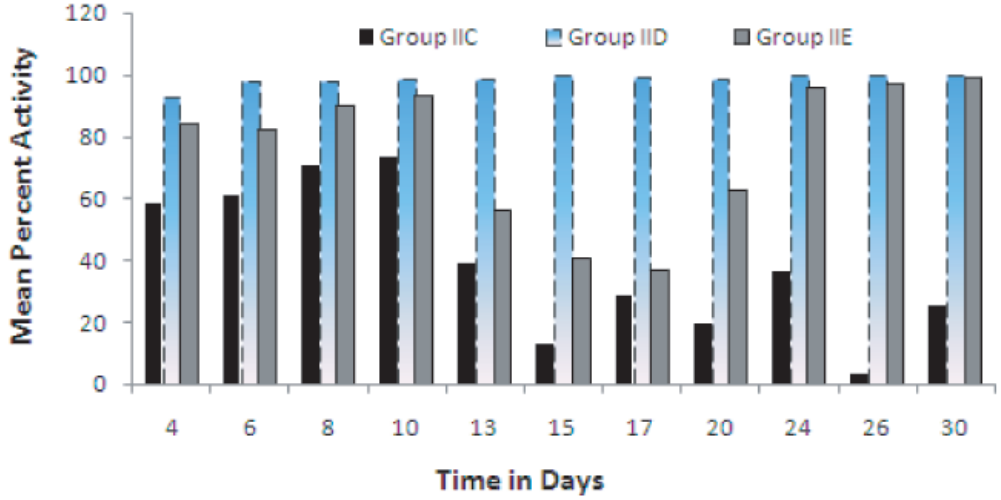

Figure 12. Antimalarial activity of lyophilized complexes of artemether in *P. berghei* infected mice (n = 6) as compared to drug.

complex, and HP-β-CD complex activity on day 1 PI were 33%, 50%, and 83.3%, respectively. However, M-β-CD (Group IIB) complexes resulted in complete clearance of the parasite from peripheral blood. Thus, the M-β-CD complex has shown a 3-fold increase in antimalarial activity compared to drug alone and the ANOVA have also shown a significant ($p < 0.05$) antimalarial activity for all the complexes compared to artemether (Figures 10-12).

4. Conclusions

In the present research work the results obtained from NMR, mass spectrometry and solution calorimetry showed a 1:1 complex of artemether with β-CD, M-β-CD, and HP-β-CD. The stability constant obtained from solution calorimetry suggested a stronger complex with M-β-CD. *In vivo* studies have shown a 3-fold increase in antimalarial activity of the lyophilized M-β-CD complex leading to the conclusion of successful development of encapsulated artemether.

Acknowledgements

The financial assistance provided by Indian Council of Medical research, New Delhi, India and the calorimeter procured under DST, New Delhi, India are gratefully acknowledged.

References

1. Balint GA. Artemisnin and its derivatives an important new class of antimalarial agents. Pharmacol Ther. 2001; 90:261-265.
2. Joshi M, Pathak S, Sharma S, Patravale V. Design and *in vivo* pharmacodyanmic evaluation of nanostructured lipid carriers for parenteral delivery of artemether: Nanoject. Int J Pharm. 2008; 364:119-126.
3. Hartell MG, Hicks R, Bhattacharjee AK, Koser BW, Carvalho K, Van Hamont JE. Nuclear magnetic resonance and molecular modeling analysis of the

interaction of the antimalarial drugs artelinic acid and artesunic acid with β-cyclodextrin. J Pharm Sci. 2004; 93:2076-2088.
4. de Araújo MV, Vieira EK, Lázaro GS, de Souza Conegero L, Ferreira OP, Almeida LS, Barreto LS, da Costa NB Jr, Gimenez IF. Inclusion complexes of pyrimethamine in 2-hydroxylpropyl-β-cyclodextrin: characterization, phase solubility and molecular modeling. Bioorg Med Chem. 2007; 15:5752-5759.
5. Jacqueline PV, Margriet G. Inclusion complexes of artemisnin or derivatives with cyclodextrins. Patent No. WO/2004075921. April, 2004.
6. Yang B, Lin J, Chen Y, Liu Y. Artemether/hydroxypropyl-β-cyclodextrin host-guest system: characterisation, phase solubility and inclusion mode. Bioorg Med Chem. 2009; 17:6311-6317.
7. Figueiras A, Ribeiro L, Torres-Labandeira JJ, Veiga Francisco JB. Evaluation of host-guest complex formation between a benzimidazolic derivative and cyclodextrins by UV-VIS spectrophotometry and differential scanning calorimetry. J Incl Phenom Macrocycl Chem. 2007; 57:531-535.
8. Ventura CA, Giannone I, Musumeci T, Pignatello R, Ragni L, Landolfi C, Milanese C, Paolino D, Puglisi G. Physico-chemical characterization of disoxaril-imethyl-β-cyclodextrin inclusion complex and *in vitro* permeation studies. Eur J Med Chem. 2006; 41:233-240.
9. Crupi V, FIcarra R, Guardo M, Majolino D, Stancanelli R, Venuti V. UV-VIS and FTIR-ATR spectroscopic techniques to study the inclusion complexes of genistein with beta-cyclodextrins. J Pharm Biomed Anal. 2007; 44:110-117.
10. Figueiras A, Carvalho RA, Ribeiro L, Torres-Labandeira JJ, Veiga Francisco JB. Solid-state characterization and dissolution characteristics on the inclusion complex of omeprazole with native and chemically modified β-cyclodextrin. Eur J Pharm Biopharm. 2007; 67:531-539.
11. Figueiras A, Ribeiro L, Vieira MT, Veiga Francisco JB. Preparation and physicochemical characterization of omeprazole: methyl-beta-cyclodextrin inclusion complex in solid state. J Incl Phenom Macrocycl Chem. 2007; 57:173-177.
12. Sinha VR, Anitha R, Ghosh S, Nanda A, Kumria R. Complexation of celecoxib with β-cyclodextrin: characterization of the interaction in solution and in solid state. J Pharm Sci. 2005; 94:676-687.
13. Chao JB, Tong HB, Liu DS, Huang SP. Preparation and characterization of inclusion complexes of pefloxacin mesylate with three kinds of cyclodextrins. Spectrochim Acta A Mol Biomol Spectrosc. 2006; 64:166-170.
14. Perry CS, Charman SA, Prankerd RJ, Chiu FC, Scanlon MJ, Chalmers D, Charman WN. The binding interaction of synthetic ozonide antimalarials with natural and modified β-cyclodextrins. J Pharm Sci. 2006; 95:146-158.
15. Torri G, Bertini S, Giavana T, Guerrini N, Puppini T, Zoppetti G. Inclusion complex characterization between progesterone and hydroxypropyl-β-cyclodextrin in aqueous solution by NMR study. J Incl Phenom Macrocycl Chem. 2007; 57:317-321.
16. Brun H, Paul M, Razzouq N, Binhas M, Gibaud S, Astier A. Cyclodextrin inclusion complexes of the central analgesic drug nefopam. Drug Dev Ind Pharm. 2006; 32:1123-1134.
17. Buchanan CM, Buchanan NL, Edgar KJ, Lambert JL, Posey-Dowty JD, Ramsey MG, Wempe MF. Solubilization and dissolution of tamoxifen-hydroxybutenyl cyclodextrin complexes. J Pharm Sci. 2006; 95:2246-2255.
18. Lahiani-Skiba M, Coquard A, Bounoure F, Verite P, Arnaud P, Skiba M. Mebendazole complexes with various cyclodextrins: preparation and physicochemical characterization. J Incl Phenom Macrocycl Chem. 2007; 57:197-201.
19. Rekharsky MV, Inoue Y. Complexation thermodynamics of cyclodextrins. Chem Rev. 1998; 98:1875-1917.
20. Royall PG, Gaisford S. Application of solution calorimetry in pharmaceutical and biopharmaceutical research. Curr Pharm Biotech. 2005; 6:215-222.
21. Higuchi T, Connors KA. Phase solubility techniques. Adv Anal Chem Instr. 1965; 4:117-212.
22. Chadha R, Kashid N, Jain DV. Characterization and quantification of amorphous content in some selected parenteral cephalosporins by calorimetric method. J Therm Anal Calorim. 2005; 81:277-284.
23. Chadha R, Kashid N, Jain DV. Microcalorimetric evaluation of the *in vitro* compatibility of amoxicillin/clavulanic acid and ampicillin/sulbatam with ciprofloxacin. J Pharm Biomed Anal. 2004; 36:295-307.
24. Kobetic R, Jursic BS, Bonnette S, Tsai SC, Salvotore SJ. Study of the lorazepam: cyclodextrin inclusion complexes using electrospray ionization mass spectrometry. Tetrahedron Lett. 2001; 42:6077-6082.
25. Cai Y, Tarr MA, Xu GX, Yalcin T, Cole RB. Studies of cyclodextrin inclusion complexes by electronic (UV-VIS absorption and emission) spectroscopy. J Am Soc Mass Spectrum. 2003; 14:449-459.
26. Djedaine F, Lin S, Perly B, Wouessidjewe D. Highfield nuclear magnetic resonance techniques for the investigation of a beta-cyclodextrin:indomethacin inclusion complex. J Pharma Sci. 1990; 79:643-646.
27. Loukas Y, Vraka V, Gregoriadis G. Use of a nonlinear least-squares model for the kinetic determination of the stability constant of cyclodextrin inclusion complexes. Int J Pharm. 1996; 144:225-231.
28. Ganza-Gonzalez A, Vila-Jato JL, Anguiano-Igea S, Otero-Espinar FJ, Blanco-Mendez J. A proton nuclear magnetic resonance of the inclusion complex of naproxen with beta-cyclodextrin. Int J Pharm. 1994; 106:179-185.
29. Zornoza A, Martin C, Sanchez M, Velaz I, Piquer A. Inclusion complexation of glisentide with α-, β- and γ-cyclodextrins. Int J Pharm. 1998; 169:239-244.
30. Yuen KH, Chan KL, Gan EK, Wong JW, Tuck TW, San Ho DS. Formulation of artemisnin. Patent No. US 2002/0147177 A1. Oct, 2002.
31. Illapakurthy AC, Sabins YA, Avery BA, Avery MA, Wyandt CM. Interaction of Artemisnin and its related compounds with hydroxypropyl-β-cyclodextrin in solution state: experimental and molecular-modeling studies. J Pharm Sci. 2003; 92:649-655.
32. Job P. Recherches sur la formation de complexes mineraux en solution et sur leur stabilite. Ann Chem. 1928; 9:113-203.

(Received January 4, 2010; Revised March 3, 2010; Accepted March 12, 2010)